PHYSICAL REVIEW A **79**, 061402(R) (2009)

Frustrated nonsequential double ionization: A classical model

K. N. Shomsky, Z. S. Smith, and S. L. Haan*
Department of Physics and Astronomy, Calvin College, Grand Rapids, Michigan 49546, USA
(Received 31 January 2009; published 2 June 2009)

Fully classical three-dimensional ensembles are examined under conditions of nonsequential double ionization and are shown to have trajectories in which both electrons apparently ionize only to have one electron bound to the nucleus after the laser pulse. These trajectories feature recollision excitation with subsequent over-the-barrier ionization at about the laser maximum. The "ionized" electron oscillates in the laser field but has small enough drift velocity to be recaptured at laser turnoff. Whether recapture can occur is shown to have extreme sensitivity to conditions at ionization.

DOI: 10.1103/PhysRevA.79.061402 PACS number(s): 32.80.Rm, 32.60.+i

Recently Nubbemeyer *et al.* [1] reported evidence of what they called "frustrated tunneling:" when helium atoms were exposed to laser pulses under conditions for tunneling ionization, nontrivial numbers of excited neutral helium atoms were produced. They explained the production of these excited atoms in terms of tunneling ionization with subsequent oscillation in the linearly polarized laser field and recapture by the Coulomb potential. These orbits are reminiscent of those discussed by Yudin and Ivanov [2], who discussed tunneling followed by long-term trapping into a Rydberg orbit.

In this Rapid Communication we consider "frustrated ionization" in a three-dimensional (3D) classical model [3] that we have employed for studying nonsequential double ionization (NSDI) [4]. The basic idea is analogous to the frustrated tunneling of Ref. [1], but the work is fully classical and features over-the-barrier ionization rather than tunneling. We focus in particular on the production of highly excited He^+ ions through a process in which both electrons apparently ionize only to have one of the electrons reattach at laser turnoff, as illustrated in Fig. 1.

A reason we consider frustrated over-the-barrier ionization in the context of NSDI rather than single ionization is the need for an effective mechanism for over-the-barrier escape. In NSDI, recollision provides the energy needed for over-the-barrier escape. However, in a fully classical one-electron atom, the electron can ionize only by "riding" a rising potential-energy curve, which leads to a very small ionization yield.

We consider laser intensity $I=0.5$ PW/cm^2 and wavelength $\lambda=800$ nm, which places the double ionization yield in the well-known "knee" area where the amount of double ionization is orders of magnitude more than would be expected if the electrons ionized independently. NSDI can be described in very classical terms [7] because the classically described laser field is strong enough to control the ionized electron's motion over almost all of its trajectory. One electron ionizes in our model over-the-barrier and due in part to energy sharing with the other electron. The oscillating laser field impels the ionized electron back to the core where "recollision" [8] leads to energy sharing and the possibility of double ionization. The simplest possibility may be impact ionization, but recollision excitation with subsequent ionization (RESI) may also occur, and experiments [9] have shown that there is not a sharp threshold for NSDI. For our model and for laser parameters presently of interest, unequal energy sharing at recollision causes RESI to be more common than direct recollision ionization even though we are above the threshold for recollision ionization [3]. The collisionally excited electron escapes the confining nuclear potential energy well during a subsequent barrier suppression, most likely the first.

It can be very difficult to find and use unambiguous terminology in describing ionization even in classical models. We present below an operational definition for ionization while the laser is still on. One could argue in favor of differ-

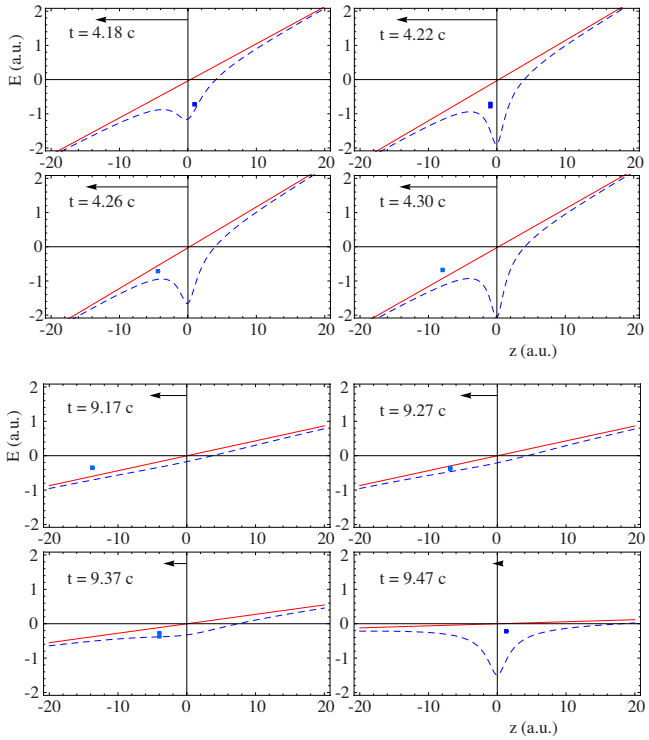

FIG. 1. (Color online) Effective energy [5,6] vs longitudinal position z. The first two rows show over-the-barrier ionization of an electron, the final two its reattachment at turnoff. By our definition, ionization occurs between $t=4.25$ and 4.26 cycle. Arrows denote laser force. The solid red curve gives the effective potential energy of the other electron, which is beyond the domain of these plots. Laser intensity is 0.5 PW/cm^2, wavelength 800 nm.

*URL: http://www.calvin.edu/~haan. haan@calvin.edu

TABLE I. Yields for 10 cycle pulses for various values of the softening parameter a. Ensemble size 2 000 000. Laser intensity 0.5 PW/cm^2 and wavelength 800 nm. SI denotes single ionization and FDI frustrated second ionization. The FDI are included in the single ionization tally.

a	SI	DI	FDI	FDI/DI*100
0.825	1 694 586	13 556	871	6.4
0.6	1 717 287	12 464	931	7.5
0.4	1 724 446	12 228	934	7.6
0.1	1 728 933	11 215	798	7.1

ent definitions, and whether at least some of the electrons should be described simply as having been excited into Rydberg orbits, such as those discussed in Ref. [2]. The main idea does not change, though: electrons that escape over the barrier as in Fig. 1 may be bound after the laser pulse is completed.

We have employed nearly the same code as for Refs. [3,10]. We populate a starting classical ensemble, with each classical atom having energy equal to the ground state of helium and with electrons moving radially. To avoid autoionization before the laser is even turned on, we replace the nuclear Coulomb potential $-2/r$ with the softened potential $-2/\sqrt{r^2+a^2}$, where $a=0.825$ (we use atomic units unless specified otherwise). We allow each atom to propagate for a time equal to one laser cycle (about 100 atomic units) before subjecting it to a sinusoidal electric field. In the present work we use ten-cycle trapezoidal pulses: two-cycle linear turn on, six cycles at full strength, and two-cycle linear turn off. One rationale for using a trapezoidal pulse is that it does not change electron drift velocity during turnoff [11]. We allow the system to propagate after the pulse for a time equivalent to one additional cycle. During the pulse, we may adjust the softening parameter a as soon as one electron exceeds a chosen distance r_a from the nucleus. This allows electrons that travel close to the nucleus at recollision to experience the large force needed for backscattering. We set $r_a=10$, and we keep the e-e shielding constant at 0.05.

One feature of these trajectories regards sensitivity to initial conditions. We have found that trajectories that are almost identical early in the pulse may diverge completely later in the pulse. This chaotic behavior has recently been quantified by Mauger *et al.* [12] for a one-dimensional (1D) system. It is very difficult to track any individual trajectory with complete confidence for the full duration of the pulse. However, the *ensemble* behavior is very stable.

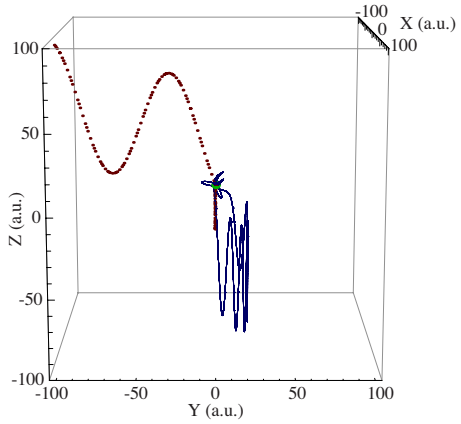

FIG. 2. (Color online) A sample two-electron trajectory from our ensemble, showing frustrated ionization. The plot begins at $t=3$ cycle. The electron represented by the solid blue curve oscillates in the laser field before reattaching to the nucleus at laser turn off. The plot continues for one laser cycle after turnoff, making the final bound orbit clearly visible.

We will use the term frustrated double ionization (FDI) to identify trajectories in which both electrons achieve a chosen minimum distance r_f from the nucleus during the pulse but after the pulse have at least one electron bound based on energy. Our results are not very dependent on the precise value of r_f. There were never more than ten trajectories in any of our ensembles that went beyond $r_f=6$ that did not also go beyond $r_f=28$. In this work we use $r_f=6$.

For laser intensity 0.5 PW/cm^2, wavelength 800 nm, and ensembles of 2×10^6 trajectories, we obtained the yield rates shown in Table I. FDI as defined above are about 7% of the DI, regardless of softening. This implies that FDI depends more on the long-range Coulomb tail than details close to nucleus. After turnoff, 90% of our FDI electrons have energy above −0.047 and 50% above −0.017. In our model it is very rare to have reattachment to He neutrals due to the ability of

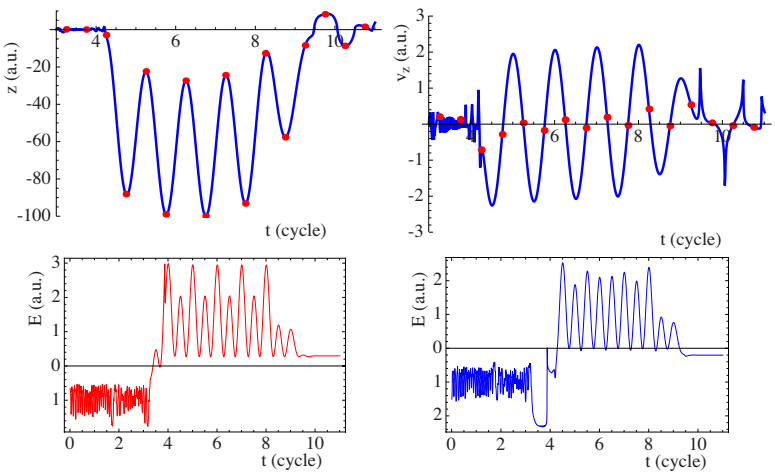

FIG. 3. (Color online) Top left: longitudinal position z vs time t (in laser cycles), for the reattaching electron of Figs. 1 and 2. Dots indicate times of field maxima ($n+0.25$ or $n+0.75$ cycle). Top right: the electron's longitudinal velocity v_z vs t. Trajectories were sampled every 0.01 cycle. Lower row: energy vs time (in laser cycles) for the trajectory of Fig. 2, on left for the electron that is free after the pulse and on right for electron that reattaches. Potential energy from interaction with laser is not included. Laser turnoff is from $t=8$ to 10 cycle. The reattaching electron finishes with energy less than zero.

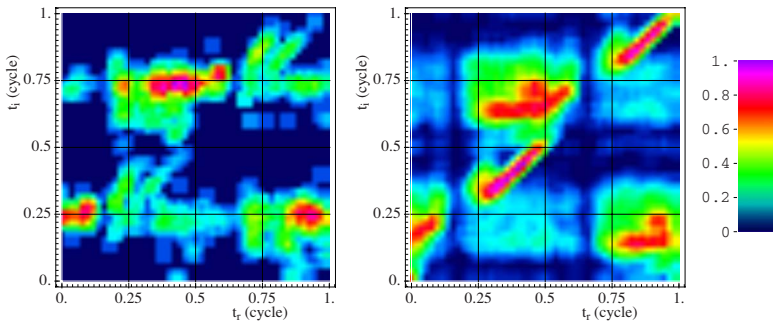

FIG. 4. (Color online) Final ionization time vs laser phase at recollision (both in laser cycles). On the left for the 934 frustrated trajectories we obtain for softening parameter $a=0.4$, and on the right for the 12 228 DI trajectories. Field maxima occur at 0.25 and 0.75 cycle. Colors are scaled independently.

the classical atoms to autoionize. (We found no more than eight in any ensemble.)

After identifying the trajectories of interest, we examine them in time steps of 0.01 cycles to find the electrons' final ionization times. Here we define an electron to be ionized if it achieves any of: $E>0$, where E is its energy, inclusive of electron nucleus and *e-e* interactions but not the laser interaction; $|z|>10$; or $zF_z>0$, with $z^2>5$ where F_z is the longitudinal component of the net force. The final test basically checks whether the net force on the electron is toward or away from the nucleus, an indicator of whether the particle is inside or outside the nuclear well. We then scan the time interval from when one electron first ionizes until the final ionization of both electrons, and we call the time of closest approach the recollision time.

For the two-electron trajectory of Fig. 1, we show the paths of the electrons in Fig. 2, starting at $t=3$ cycle. In Fig. 3 we show the longitudinal position and velocity vs time for the reattaching electron. We also show the electron energies, excluding the electron-laser potential energy. This trajectory is from the ensemble for $a=0.825$. One electron ionizes at $t=3.35$ cycle and travels out from the core to $z=-29$, then comes back and collides with the other electron at $t=3.87$ cycle. The returning electron gives up only a portion of its energy, in fact maintaining enough so that it can drift out in the forward direction after recollision. We consider forward drift in more detail in Ref. [10]. The struck electron oscillates in the well until emerging over the barrier at 4.26 cycle. It then executes much larger oscillations in the laser field until laser turnoff when it reattaches to the nucleus. The plots continue for one cycle after laser turnoff so the bound motion of the electron is visible. Because of the large Coulomb softening, the final motion visible in Fig. 2 is not elliptical.

We now consider ensemble properties of the FDI trajectories. The left side of Fig. 4 plots laser phase at final ionization vs laser phase at recollision (both in laser cycles) for the 934 frustrated trajectories we obtain for softening parameter $a=0.4$. A plot for DI trajectories from the same ensemble is shown on the right [13], color coded independently. The plots allow for wraparound. Only a small number of the frustrated trajectories lie along the diagonal, thus allowing us to associate the frustrated trajectories with RESI. (An equivalent plot for $a=0.825$ would not have any trajectories on the diagonal.) Final ionization occurs most often at times nearly equal to a laser maximum ($t_i=0.25$ or 0.75 cycle), slightly later than for the RESI trajectories of the right-hand plot. A quick check confirms that most of the final ionizations occur in the first field maximum after ionization.

Energies of the two electrons 0.06 cycle after recollision are shown in Fig. 5. We consider FDI trajectories on the left and DI trajectories on the right. The recolliding electron very often has positive energy after recollision, the struck electron negative, though the energy transfer may be so large that it is the recolliding electron that is bound after the collision. There is also notable probability of a doubly bound state. There is no region of the plot that is unique to the FDI trajectories and thus able to serve as a predictor of FDI.

In Fig. 6 we plot the longitudinal velocity vs laser phase at the time of final ionization for $a=0.4$. On the left we consider FDI electrons and on the right the second electron to achieve final ionization in DI pairs. The region that can lead to frustrated ionization is limited but not unique to FDI, so again we have no predictor.

To investigate the apparent absence of predictors of FDI, we employ the familiar 1D Rochester potential [14] for Z $=2$, $V(x)=-2/\sqrt{1+x^2}$. We launch an electron outward from the cusp at the time of a laser maximum with velocity v_0 for

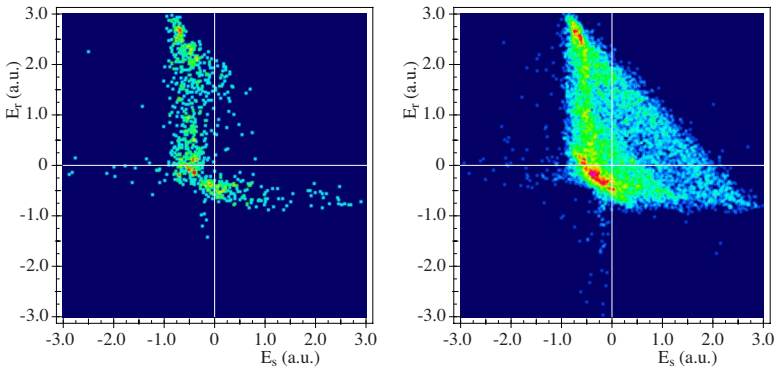

FIG. 5. (Color online) Energy E_r of the recolliding electron vs energy E_s of the struck electron 0.06 cycle after recollision. FDI trajectories are on the left, and DI on the right; $a=0.4$. Colors are scaled independently. No region is unique to FDI.

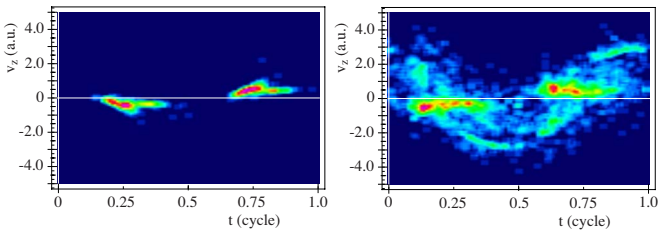

FIG. 6. (Color online) Longitudinal velocity at ionization vs laser phase (in cycles) at final ionization, for softening parameter $a=0.4$. Left: FDI electrons. Right: the second electron to ionize in DI trajectories.

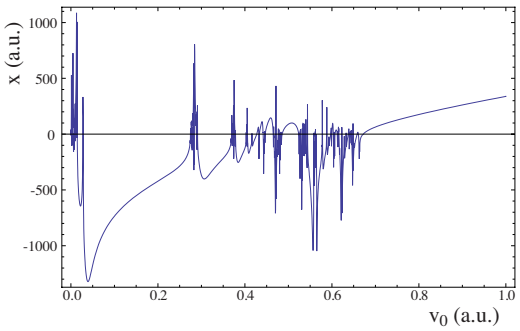

FIG. 7. (Color online) Electron position x at time 5 laser cycles after launch vs starting velocity v_0, in a 1D model. The electron begins at the cusp (near $x=3.9$) at the time of a laser maximum. The final position of the electron has extreme sensitivity to initial velocity, explaining why there is no simple predictor for FDI.

the same laser frequency and ponderomotive energy as above. We solve its equation of motion and consider in particular its position 5 cycles after launch. We plot the position x vs v_0 in Fig. 7. For initial velocities above about 0.7, the electron drifts out in the direction of its escape. However, for smaller launch velocities there are regions where it could go either into the positive or negative regions or be near the nucleus. In short, it is a nonlinear system with extreme sensitivity to initial conditions. Because of this chaotic behavior, we do not have well separated regions of phase space at ionization leading to different final conditions.

Reattachment of an ionized electron at laser turnoff has been discussed also within the context of stabilization [15] in superintense fields. Its classical nature was discussed in Ref. [16].

In summary, we have shown that electrons that escape the nuclear well or in other ways test out as ionized in classical models may be bound at the end of the pulse. These electrons can be described as having small enough drift velocity that they are near the nucleus and traveling slowly at laser turnoff. Electrons that subsequently reattach are most likely to be the result of RESI and to have escaped at about the time of a field maximum, but whether a specific trajectory leads to reattachment in this nonlinear system is extremely sensitive to its velocity at the time of ionization.

This material was based upon work supported by the National Science Foundation under Grant No. 0653526 to Calvin College. This work was an outgrowth of a collaboration with J. H. Eberly's group at the University of Rochester. We also acknowledge discussions with A. K. Das, computer assistance from P. W. Plantinga, and support from Calvin College.

[1] T. Nubbemeyer, K. Gorling, A. Saenz, U. Eichmann, and W. Sandner, Phys. Rev. Lett. **101**, 233001 (2008).

[2] G. L. Yudin and M. Y. Ivanov, Phys. Rev. A **63**, 033404 (2001); see also T. Brabec, M. Y. Ivanov, and P. B. Corkum, *ibid.* **54**, R2551 (1996).

[3] S. L. Haan, L. Breen, A. Karim, and J. H. Eberly, Phys. Rev. Lett. **97**, 103008 (2006); Opt. Express **15**, 767 (2007).

[4] For reviews of NSDI, see R. Dörner *et al.*, Adv. At., Mol., Opt. Phys., **48**, 1 (2002); A. Becker, R. Dörner, and R. Moshammer, J. Phys. B **38**, S753 (2005); A. Becker and F. H. M. Faisal, *ibid.* **38**, R1 (2005).

[5] Effective energy diagrams were introduced in Ref. [6]. Here, as in the second part of Ref. [3], we plot the effective potential-energy curves in terms of only the z coordinate. The shape changes due to parametric dependence on x and y. Thus, for example, the nuclear well is evident only if x and y are small.

[6] R. Panfili, S. L. Haan, and J. H. Eberly, Phys. Rev. Lett. **89**, 113001 (2002).

[7] P. J. Ho, R. Panfili, S. L. Haan, and J. H. Eberly, Phys. Rev. Lett. **94**, 093002 (2005).

[8] P. B. Corkum, Phys. Rev. Lett. **71**, 1994 (1993); K. J. Schafer, B. Yang, L. F. Di Mauro, and K. C. Kulander, *ibid.* **70**, 1599 (1993).

[9] E. Eremina *et al.*, J. Phys. B **36**, 3269 (2003).

[10] S. L. Haan, Z. S. Smith, K. N. Shomsky, and P. W. Plantinga, J. Phys. B (in press), e-print arXiv:0901.2554.

[11] R. Grobe and M. V. Fedorov, Phys. Rev. Lett. **68**, 2592 (1992).

[12] F. Mauger, C. Chandre, and T. Uzer, Phys. Rev. Lett. **102**, 173002 (2009).

[13] A similar plot appears in Fig. 2 of Ref. [10] but for a 5 cycle laser pulse. The primary effect of increasing the pulse length is to favor RESI from recollisions occurring at about the time of a laser zero.

[14] J. Javanainen, J. H. Eberly, and Q. Su, Phys. Rev. A **38**, 3430 (1988); J. H. Eberly, *ibid.* **42**, 5750 (1990).

[15] J. I. Gersten and M. H. Mittleman, J. Phys. B **9**, 2561 (1976); M. Gavrila and J. Z. Kaminski, Phys. Rev. Lett. **52**, 613 (1984); Q. Su, J. H. Eberly, and J. Javanainen, *ibid.* **64**, 862 (1990).

[16] R. Grobe and C. K. Law, Phys. Rev. A **44**, R4114 (1991).